International Journal of Minerals, Metallurgy and Materials
Accepted manuscript, https://doi.org/10.1007/s12613-024-3066-6

Rapid identification method for evaluating high-purity quartz

Min Liu[1)], *Guocheng Lv*[2),✉], *Xin Liu*[2)], *Zijie Ren*[3),✉], *Meitang Liu*[2)], *Ritong Huang*[2)], *Xinyu Hou*[2)], *Qinwen Zheng*[2)], *Libing Liao*[2)], *and Jingwen Mao*[4)]

1) School of Earth Sciences and Resources, China University of Geosciences, Beijing 100083, China

2) Engineering Research Center of Ministry of Education for Geological Carbon Storage and Low Carbon Utilization of Resources, Beijing Key Laboratory of Materials Utilization of Nonmetallic Minerals and Solid Wastes, National Laboratory of Mineral Materials, School of Materials Science and Technology, China University of Geosciences, Beijing 100083, China

3) Key Laboratory of Green Utilization of Critical Non-metallic Mineral Resources, Ministry of Education, Wuhan University of Technology, School of Resources and Environmental Engineering, Wuhan University of Technology, Hubei Province Key Laboratory of Processing of Mineral Resources and Environment, Wuhan 430070, China

4) MNR Key Laboratory of Metallogeny and Mineral Assessment, Institute of Mineral Resources, Chinese Academy of Geological Sciences, Beijing 100037, China

✉Corresponding authors: Guocheng Lv E-mail: guochenglv@cugb.edu.cn; Zijie Ren E-mail: renzijie@whut.edu.cn

Abstract: The rapid growth of semiconductor, photovoltaic, and other emerging industries has led to a sharp increase in demand for high-purity quartz in China, particularly for 4N5-grade (99.995% SiO_2) and above. However, the heavy reliance on imported high-purity quartz poses a significant risk to the security of key national strategic industries. To address this challenge, China is focusing on identifying domestic sources of high-purity quartz and developing efficient evaluation methods. This study investigates the inclusion content in three types of quartz: pegmatite, vein quartz, and white granite. A grading system based on the transmittance of quartz grains was established by analyzing the number of inclusions. Five quartz ore samples from different regions were purified, and the resulting concentrates were analyzed using inductively coupled plasma mass spectrometry (ICP). The relationship between the inclusion content of raw quartz, the composition of the purified quartz, and the quality of the sintered fused quartz products was examined. The findings demonstrate that quartz with fewer inclusions results in lower impurity levels after purification, higher SiO_2 purity, and the more translucent the glass, as confirmed by firing tests. Herein, This study establishes a clear connection between quartz inclusions and the

overall quality of high-purity quartz. The proposed approach enables rapid assessment of quartz deposit quality by identifying inclusions, offering a practical and efficient method for locating high-quality quartz resources.

Keywords: High-purity quartz, Grading, Inclusions, Rapid evaluation

1. Introduction

High-purity quartz is an essential material widely used in semiconductors, optical fibers, photovoltaics, aerospace, military technology, laboratory equipment, and other advanced fields [1-5]. Its critical role in these industries makes it highly sought after, with demand continuing to grow rapidly as global science and technology advance [6-7]. However, the number of deposits capable of producing high-purity quartz is limited and unevenly distributed worldwide [8]. Currently, China relies heavily on imports of high-purity quartz (above 4N5 grade) for strategic applications. To reduce this dependency, there is an urgent need to identify domestic sources of high-quality quartz quickly and efficiently.

High-purity quartz is distinguished by an exceptionally high SiO_2 content compared to standard quartz. The international standard for high-purity quartz requires a minimum SiO_2 concentration of 99.995% [9]. In addition to SiO_2, trace amounts of impurity elements such as Al, Ca, Co, Cr, Cu, Fe, K, Li, Mg, Mn, Na, Ni, and Ti, as well as small molecules like CO_2 and H_2O, are present in high-purity quartz [10-11]. According to the standards for IOTA-series products from Sibelco North America (formerly Unimin), among these13 key impurity elements, Al and Ti typically have slightly higher concentrations, ranging from (7-16.2) μg g^{-1} and (1.1-1.4) μg g^{-1}, respectively, while the concentrations of the other impurities are below 1.0 μg g^{-1} [12]. To qualify as high-purity quartz, the total impurity content must be less than 19.66 μg g^{-1}, and the SiO_2 purity must exceed 99.998%. These high-grade quartz products are the most in demand globally [13]. Müller *et al.* established additional concentration limits for harmful elements in high-purity quartz sourced from Norwegian deposits [14]. The maximum allowable concentrations include: Al<30 μg g^{-1}, Ti<10 μg g^{-1}, Na<8 μg g^{-1}, K<8 μg g^{-1}, Li<5 μg g^{-1}, Ca<5 μg g^{-1}, Fe<3 μg g^{-1}, P<2 μg g^{-1}, B<1 μg g^{-1}, with the total concentration of these elements not exceeding

50 μg/g. In response to evolving domestic and international market demands, Wang *et al*. proposed a refined classification for high-purity quartz in China based on SiO_2 purity levels [15]. These include high-end quartz with SiO_2 ≥99.998% (4N8), middle- and high-end quartz with SiO_2 ≥99.995% (4N5), mid-range quartz with SiO_2 ≥99.99% (4N), and low-end quartz with SiO_2 ≥99.9% (3N). This classification highlights the importance strict impurity control to meet the demands of high-purity quartz in advanced applications. With rising global demand, efficiently evaluating and developing high-quality quartz resources is essential to reducing import reliance and ensuring a stable supply for industries.

Table 1. Classification of high-purity quartz products and quality requirements for raw ore material

Classification	High-end	Mid-to-high-end	Mid-end	Low-end
ω(SiO_2)	⩾99.998% 4N8	⩾99.995% 4N5	⩾99.99% 4N	⩾99.9% 3N
Impurity content	⩽20 μg g^{-1}	⩽50 μg g^{-1}	⩽100 μg g^{-1}	⩽1000 μg g^{-1}
Grain size	40-8 mesh, 80-140 mesh, 100-200 mesh, 80-300 mesh, etc.			
Current state of the technology	Imported mainly from the United States, Norway, etc.	Basic localization	Localization	Localization
Ore material grade	Grade A ore High-quality mines or high-quality raw materials	Grade B ore Top-quality ore or top-quality raw materials	Grade C ore Medium ore or medium raw material	Grade D ore Inferior ore or inferior raw materials

The data in this table is quoted from [15].

Impurities in high-purity quartz primarily originate from fluid inclusions within the quartz, with some impurities present in the quartz lattice as well. These impurities significantly affect the quality and performance of the quartz [16-18]. For example, metallic impurities can affect the electrical properties of semiconductor devices, while

gas-liquid inclusions create bubbles at high temperatures, reducing the transparency of optical components [18-19]. In natural quartz, some of these impurities can be removed by various purification strategies to increase the SiO_2 content [11, 20, 21]. Purification methods are generally categorized into physical and chemical processes. Physical methods include crushing, magnetic separation, and calcination with water quenching, flotation is a physicochemical method, while chemical methods primarily involve acid leaching and chlorination roasting [22-23].

Quartz inclusions are typically grouped into mineral inclusions, primary fluid inclusions formed during ore genesis, and secondary fluid inclusions trapped during later geological events [24]. The type, number, and size of these inclusions vary depending on the quartz's origin and type, leading to differences in high-purity quartz quality [25]**Error! Reference source not found.**. It is known that inclusions are a major factor influencing impurity levels. Therefore, the quality of high-purity quartz can be effectively assessed by analyzing its inclusion content [26].

In this study, we analyzed natural high-purity quartz ores from different types, *i.e.*, pegmatite-type, vein quartz-type, and white granite-type, sourced from the regions of Xinjiang, Shanxi, and Gansu. The quality of the quartz ores was preliminarily assessed by observing and statistically analyzing the inclusions, and grading criteria were established based on these observations. Subsequently, purified quartz concentrates were then analyzed for impurity composition and subjected to melting tests to explore the relationship between inclusion content, impurity levels, and melting performance. The results indicate that lower inclusion content led to higher purity in the purified quartz concentrates, as well as improved glass transparency and fewer bubbles after firing. These findings confirm the feasibility of the inclusion-based rapid evaluation methods assessing high-purity quartz quality. This approach provides a practical tool for efficiently exploring, developing, and utilizing high-purity quartz resources, offering a strong technical foundation for future quartz prospecting in China.

2. Experiments and Materials

2.1 Experimental materials

The five natural quartz samples in this study were sourced from Xinjiang, Gansu, and Shanxi. Dodecylamine collector ($C_{12}H_{27}N$, 10 g/L) was purchased from Sinopharm Group *Co. Ltd*., while hydrofluoric acid (HF, 10 mol/L), an anion trapping agent, and a cation trapping agent were purchased from Wuhan Qingjiang Chemical Huanggang *Co. Ltd.*, and the refractive oil was a self-prepared mixture. All chemicals were of analytical grade and were used without further purification.

2.2 Quartz inclusions identification method

Firstly, the quartz raw ore was crushed, and fresh quartz grains were selected, minimizing interference from impurity minerals. After grinding, the samples were sieved through a 60-140 mesh screen, washed, dried, and placed in slide grooves, submerged in mixed oils. The samples were evenly spread to avoid stacking and then observed under the optical microscope. Microscopic images were captured with the magnification of 50. Multiple images were taken at different coordinates, ensuring no duplicate grains were photographed. Finally, several images were selected to identify inclusions in quartz samples from different regions.

2.3 Purification of quartz

Fig. 1 shows a flow chart of the complete purification process.

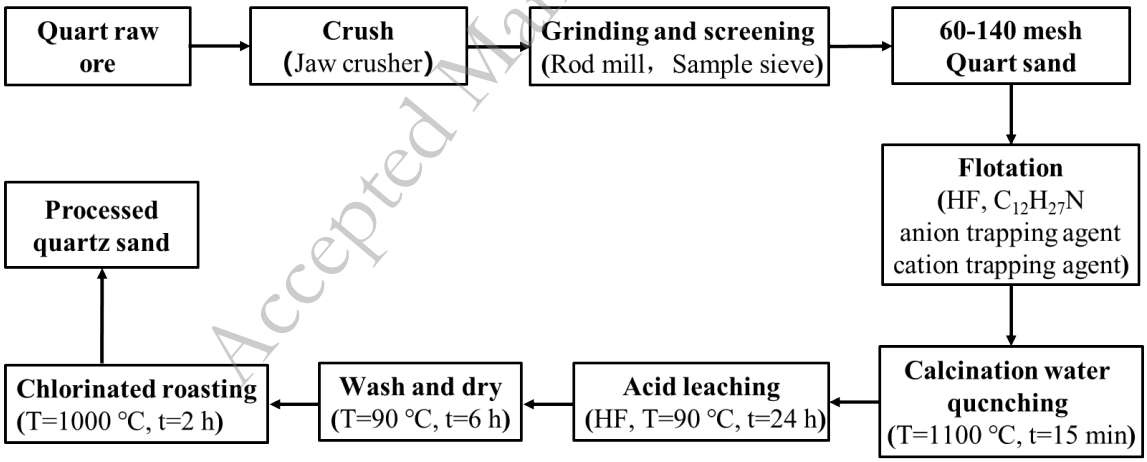

Fig. 1. Flow chart of purification process

(1) Crushing

The raw ore was crushed using a PE100 jaw crusher. The ore was then ground using an RK/BM three-roller and four-cylinder intelligent rod mill. After grinding, the adhering soil was washed off, and the ore was screened through a standard nylon

sieve to collect 60-140 mesh grains. The ore was baked at 90°C for 3 h and then used for magnetic separation to remove magnetic minerals.

(2) Flotation process

A 0.5L XFD-IV flotation machine was used to remove feldspar, mica, and other impurities. The pH was adjusted to 2-3 using an HF solution, and 0.5 mL of dodecylamine collector was added. The mixture was stirred for 3 minutes and then opened the inflation valve for 30 s. For the second flotation, the pH was adjusted to 1.5~2 using HF, and 0.5~1 mL each of anion and cation trapping agents were added. The mixture was stirred for 3 min before opening the inflation valve. The separation principle is mainly based on the different Zeta potentials of mica, feldspar, and quartz. HF is used to adjust the pH to near the zero point of quartz, where the quartz surface is not charged, and other impurities have a positive or negative surface charge. Cation collectors or a combination of cation and anion collectors can be used to electrostatically or selectively adsorb on the impurity minerals surface, which makes the surface of the impurity minerals be hydrophobic, thus enhancing its floatability. Therefore, the effective separation of quartz from feldspar, mica and other impurity minerals can be achieved through the electrostatic attraction or complexation between the collectors and the surface of impurity minerals [27].

After flotation, the quartz sand was washed via ultrasonic agitation at 80 °C, then dried for 8 hours at 40-50 °C.

(3) Calcination and water quenching

The SX2-2.5-10 muffle furnace was preheated to 1100°C, and the flotation quartz sand was heated in the furnace for 15 minutes. The calcined quartz was then quickly poured into a beaker containing deionized water, washed, filtered, and dried in preparation for acid leaching.

(4) Acid leaching

The quartz sand was placed in the PTFE lining of the reactor, and 4% HF solution was added. Hydrothermal acid leaching was conducted at 90°C for 24 h. After leaching, the samples were washed until neutral pH was achieved, then dried in an oven at 40-50°C for 8 h.

(5) Chlorinated roasting

The quartz sand was evenly spread in a quartz boat and placed in the chlorination roaster. The roaster was set to 1000 °C, with the gas being changed every 15 min for a total duration of 110 min.

2.4 Quartz melting method

The purified and dried high-purity quartz sand was placed in a quartz glass tube and heated above its melting point using a hydroxide flame. Once the quartz melted into a liquid state, it was cooled to form a fused quartz crystal glass tube.

2.5 Characterization method

For inclusion observation, an Axioscope 5 polarizing microscope (Zeiss) was used, and sample images were captured using an Axiocam 506 color large-area imaging camera. Thirteen trace element contents of Al, Ca, Co, Cr, Cu, Fe, K, Li, Mg, Mn, Na, Ni, and Ti were detected using a NexION 1000 inductively coupled plasma mass spectrometer (PerkinElmer Company, USA).

3. Results and discussion

3.1 Inclusion body evaluation system

Quartz inclusions can be categorized into several distinct types, each exhibiting unique shapes and characteristics. The primary classifications include daughter mineral inclusions, melt inclusions, and fluid inclusions. These inclusions provide valuable insights into the geological history and formation conditions [28-29]. These fluid inclusions are most common and are further divided into different types based on their structures. Single-phase saline solution inclusions are typically shaped like rice grains, ellipsoids, polygons, or irregular forms. Single-phase gas-phase inclusions mostly appear as rounded bubbles. Gas-liquid two-phase inclusions containing CO_2 are commonly elliptical, rounded, polygons, or short rectangular in shape. Two-phase saline solution inclusions are mainly ellipsoidal or negatively crystalline, with some displaying semi-automorphic negatively crystalline structures [30-32].

Quartz rocks from different regions exhibit notable differences in their external and internal characteristics. Generally, quartz with higher transparency contains fewer inclusions [28]. This relationship between transparency and inclusion content is an

important visual indicator of quartz quality. By studying the characteristics of quartz ores and their inclusions, and taking into account practical application requirements, a grading system for high-purity quartz was developed based on the percentage of permeable grains. This system classifies quartz into four grades: A, B, C, and D. Class A quartz, modeled after quartz sourced from the Spruce Pine District, North Carolina, USA, is of exceptionally high purity and contains very few mineral inclusions [33-34]. Class B quartz, based on Indian quartz sources, also exhibits high purity but contains slightly more inclusions [35]. Class C quartz is derived from pegmatites in Xinjiang [36], and contains a higher number of inclusions. Class D quartz, based on vein quartz from Gansu, shows a very high inclusion content, making it easy to distinguish.

To enable the rapid evaluation of high-purity quartz rocks, a statistical method was developed. In this method, all quartz grains within the field of view are analyzed. Permeable quartz grains are defined as those with no internal black dots visible under 50x magnification. Semi-permeable grains contain a small number of internal black dots, while impermeable grains have many internal black dots or visible mineral inclusions. However, the specific types of mineral inclusions are not counted. Quartz grains in the field of view are categorized into grades A, B, C, or D by calculating the percentage of permeable grains. For individual quartz grains, the inclusion content is used to determine transmittance. Permeable quartz grains should possess an inclusion percentage of less than 0.25%. Semi-permeable grains exhibit inclusion percentages between 0.25% and 4%, while impermeable grains present inclusion percentages exceeding 4%. Fig. 2 outlines the specific grading standards, showing that quartz quality decreases from grade A to grade D as the inclusion content increases. Table 2 provides the detailed evaluation method for assessing the transmittance of all quartz grains in the observed field.

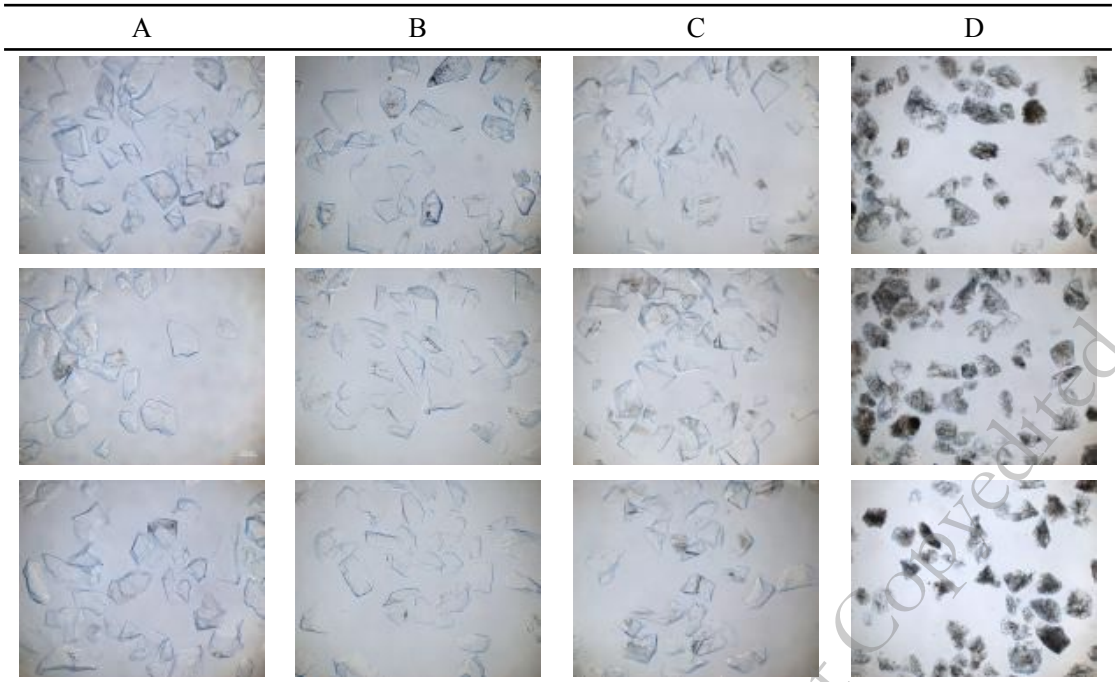

Fig. 2 Grading criteria data card.

Table 2. Data on classification criteria.

Translucent grains / Impermeable grains	⩾65%	⩾45%	⩾30%	⩾0%
⩽2%	A	B	C	C
⩽8%	B	B	C	C
⩽20%	B	B	C	D
⩽35%	C	C	C	D
⩽55%	/	C	D	D
⩽70%	/	/	D	D
⩽100%	/	/	/	D

3.2 Evaluation results of different types of high-purity quartz inclusions

3.2.1 White granite

Fig. 3(a) shows a picture of a white granite ore sample from a region in Xinjiang,

sample number 1. The sample was crushed to about 10 mesh, and the quartz monomineral grains were selected, and the quartz sample grains with granularity between 60-140 mesh were washed after crushing and sieving for testing. Appropriate amount of treated quartz grains were evenly dispersed on a 22 × 22 cm slide with grooves to ensure that the quartz grains were flat and did not overlap, and then refractive oil was added onto the slide to complete the preparation. After microscopic observation, it was concluded that the inclusions were: translucent quartz grains accounted for 50% of all quartz grains (45% or more of class B quartz), opaque quartz grains accounted for 6% of all quartz grains (6% or less of class B quartz), and the rest were semi-transparent quartz grains (as shown in Fig. 3(b-e)). The sample is thus judged to be Class B quartz.

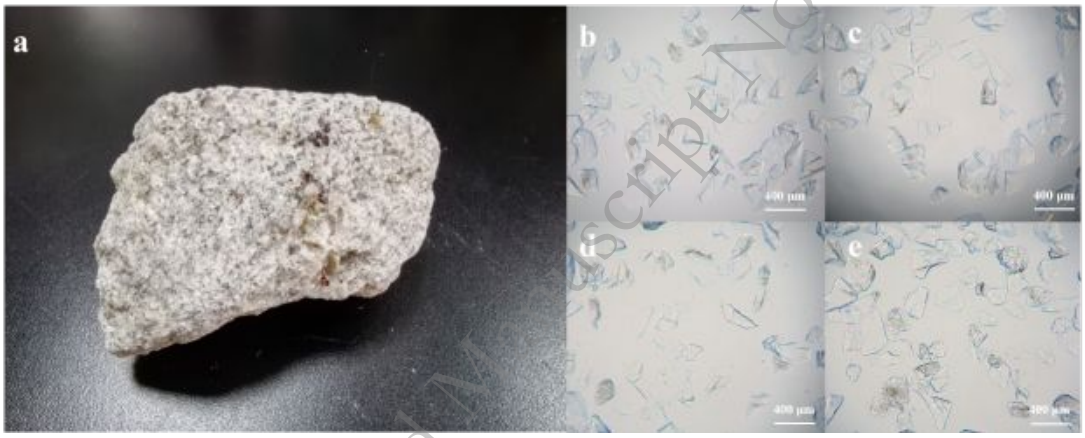

Fig. 3. Photograph of raw ore (a) and microscopic images (b-e) of sample No.1

Fig. 4(a) shows a photograph of an white granite ore sample from a region in Xinjiang, referred to as Sample No.2. The ore was prepared following the same procedure as the pegmatite sample. Quartz grains were separated, homogenized, sieved to the desired grain size (60–140 mesh), washed, air-dried, and prepared for testing. Microscopic examination of this sample showed that 41% of the quartz grains were translucent, satisfying the requirement of 30% or more for Class C quartz. Furthermore, 12% of the grains were impermeable, meeting the requirement of 20% or less for Class C quartz, while the remaining grains were semi-permeable, as shown in Fig. 2(b-e). This sample was determined to have a moderate inclusion content,

which affects its quality, and was consequently classified as Class C quartz.

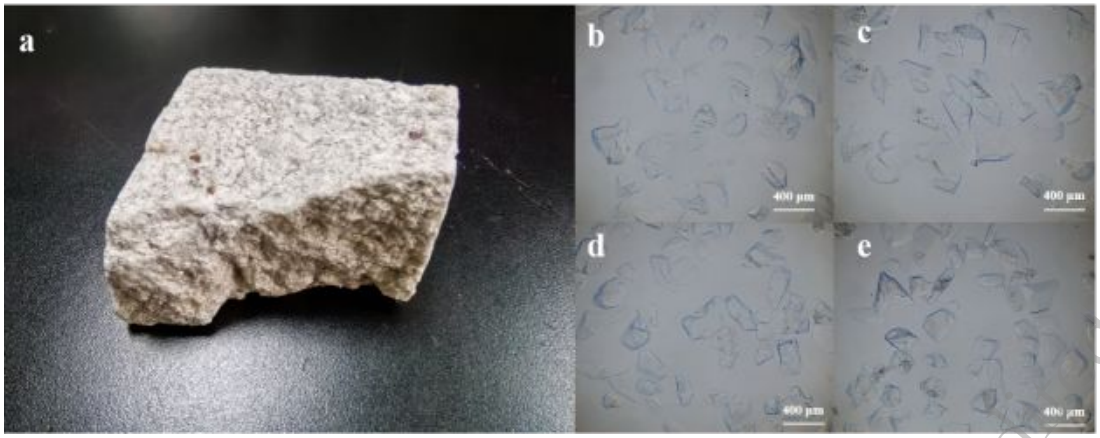

Fig. 4. Photograph of raw ore (a) and microscopic images (b-e) of Sample No.2.

3.3.2 Pegmatite

Fig. 5(a) shows a photograph of a pegmatite ore sample from a region in Xinjiang, referred to as Sample No.3. The ore was crushed to a grain size of approximately 8-10 mesh, and individual quartz grains were selected, further crushed, and sieved to obtain samples with a grains size range of 60–140 mesh. These samples were then washed and prepared for testing. A small amount of the treated quartz grains was evenly dispersed on a 22×22 cm fluted slide to ensure that the grains were flat and non-overlapping. Refractive oil was then added to complete the sample preparation process. Microscopic analysis revealed that 44% of the quartz grains were translucent, with over 30% meeting the criteria for Class C quartz. Additionally, 10% of the grains were opaque, with less than 20% meeting the criteria for Class C quartz, while the remaining grains were semi-translucent, as shown in Fig. 5(b-e). Based on these findings, the sample was classified as Class C quartz due to its moderate inclusion content.

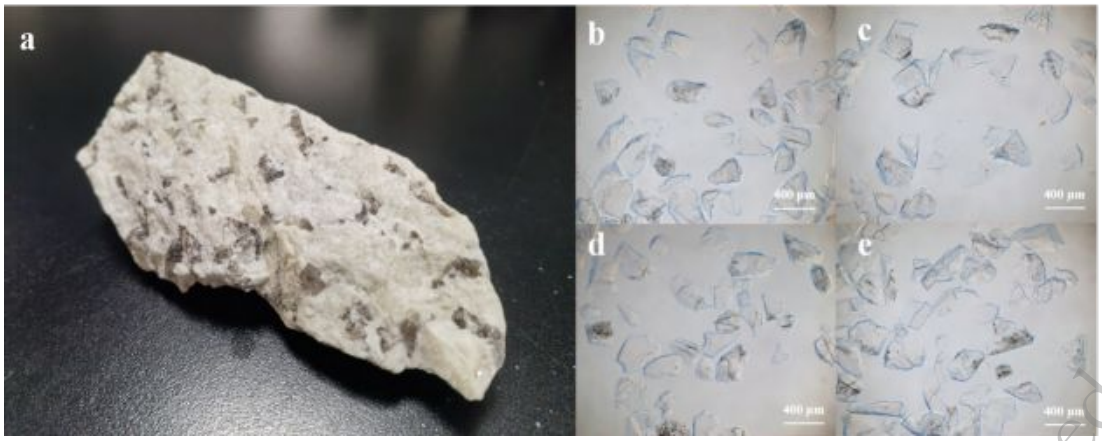

Fig. 5. Photograph of raw ore (a) and microscopic images (b-e) of sample No.3.

3.2.3 Quartz vein

Fig. 6(a) shows a photograph of a vein quartz sample from Gansu, referred to as Sample No.4. The raw ore was crushed, and individual quartz grains were separated, homogenized, sieved (60-140 mesh), washed, air-dried, and prepared for testing. Optical microscopy was used to observe the sample and analyze its inclusion content. The analysis revealed that only 17% of the quartz grains were permeable, while more than 34% of the grains were impermeable. The remaining grains were classified as semi-permeable, as shown in Fig. 6(b-e). The high inclusion content and low transparency indicated poor mineral quality, and the sample was classified as Class D quartz.

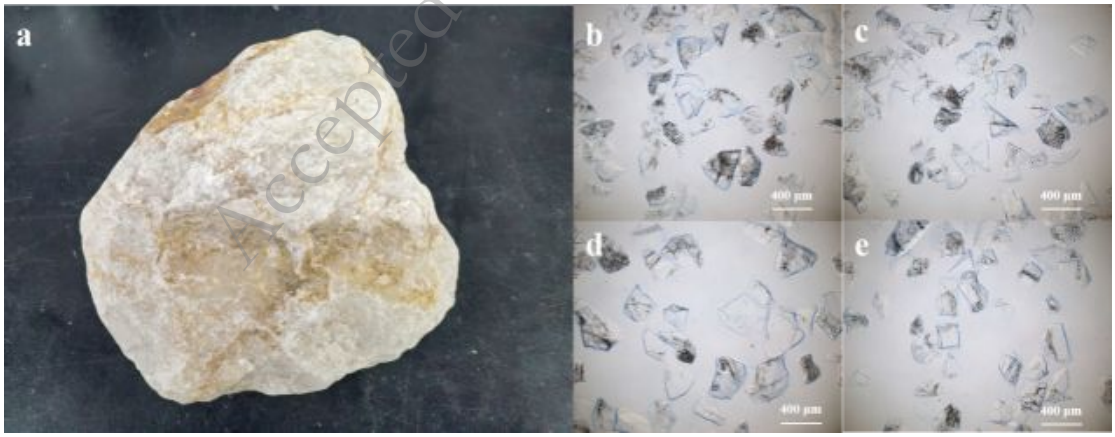

Fig. 6. Photograph (a) and microscopic images (b-e) of the raw ore of sample No.4.

Fig. 7(a) shows a vein quartz sample from Shanxi, referred to as Sample No.5. After sieving and pre-treatment, the sample was analyzed under a microscope. The results revealed that none of the quartz grains were permeable, while over 80% were

impermeable, indicating a high inclusion content, as shown in Fig. 7(b-e). Based on these observations, the sample was classified as Class D quartz due to its very high inclusion content and poor mineral quality.

Fig. 7. Photograph of raw ore (a) and microscopic images (b-e) of Sample No.5.

The quality of quartz rocks can be preliminarily assessed by observing the inclusion content and other characteristics under a microscope. Sample No.1 has 50% permeable grains and 6% impermeable grains, which is classified as B quartz. No.2 has 41% permeable grains and 12% impermeable grains, which belongs to the range of class C quartz. For Sample No.3, 44% of the grains were permeable, and 8% were impermeable. This places the sample in Class C quartz, though it is close to meeting the criteria for Class B quartz. In contrast, Sample No.4 presented only 17% permeable grains and 34% impermeable grains, resulting in its classification as Class D quartz, due to its higher inclusion content and poorer mineral quality. Similarly, Sample No.5 contained no permeable grains and more than 80% impermeable grains, confirming its classification as Class D quartz. These results highlight the variation in inclusion content among different types of quartz rocks and demonstrate the effectiveness of the grading criteria established in this study. Table 3 provides a detailed summary of the grading results and their alignment with the proposed classification standards.

Table 3. Classification grades of high-purity quartz samples.

Sample number	1	2	3	4	5
Grade Classification	B	C	C	D	D
Translucent grains (%)	50	41	44	17	0
Semi-permeable grains (%)	44	47	46	49	20
Impermeable grains (%)	6	12	10	34	80

3.3 Impurity composition analysis of different types of high-purity quartz

After purifying five types of quartz raw ore samples, the resulting quartz concentrates were analyzed for 13 impurity elements, *i.e.*, Al, Ca, Co, Cr, Cu, Fe, K, Li, Mg, Mn, Na, Ni, and Ti. The results, presented in Table 4, show that SiO_2 is the primary component in all the samples. The SiO_2 content of sample No.1 is 99.997%, and the total amount of thirteen impurity elements is 21.8 μg g^{-1},which contains 12.86 μg g^{-1} of Al, 5.11 μg g^{-1} of Ti, which was the lowest impurity content and the highest purity among these five samples. The SiO_2 content of sample No.2 is 99.997%, and the total amount of thirteen impurity elements is 28.77 μg g^{-1}, which contains 20.42 μg g^{-1} of Al, 2.82 μg g^{-1} of Ti, and a small number of other elements. The elemental components sample No.1 and sample No.2 fall within the elemental limits for high-purity quartz as proposed by Müller (2012) for Norwegian deposits. The SiO_2 content of Sample No.3 is 99.997%, with a total impurity concentration of 25.72 μg g^{-1}. Among these impurities, Al accounts for 15.65 μg g^{-1}, Ti for 5.52 μg g^{-1}, and the remaining elements are present in smaller amounts. These values also meet the impurity limits for high-purity quartz defined by Müller (2012) for Norwegian deposits, and the SiO_2 content satisfies the 4N7 product standard.

In contrast, Sample No.4 has a slightly lower SiO_2 content of 99.995% and a total impurity concentration of 41.26 μg g^{-1}. The Al content is relatively high, reaching 33.53 μg g^{-1}, while Ti accounts for 3.35 μg g^{-1}. Although the SiO_2 content meets the high-purity quartz standard, the elevated Al concentration exceeds Müller's limits, making it unsuitable for high-purity quartz applications. Sample No.5 has the lowest SiO_2 content among the four samples at 99.994%, with a total impurity

concentration of 55.42 mg/kg. This includes 21.12 μg g^{-1} of Al and 17.91 μg g^{-1} of Ti, both of which exceed Müller's permissible limits for high-purity quartz. Despite the high SiO_2 content of samples 4 and 5, the elevated levels of Al, Ti, and other impurities prevent Sample No.4 and No.5 from meeting international standards for high-purity quartz.

Table 4. Full plasma emission spectroscopy analyses (ICP) of five quartz concentrate products.

Element	1	2	3	4	5
Al(μg g^{-1})	12.86	20.42	15.65	33.53	21.12
Ca(μg g^{-1})	1.10	2.35	1.00	0.77	4.65
Co(μg g^{-1})	0.01	0.01	0.01	0.01	0.04
Cr(μg g^{-1})	＜0.01	0.01	＜0.01	0.01	0.11
Cu(μg g^{-1})	0.02	0.03	0.03	0.01	0.04
Fe(μg g^{-1})	0.07	0.52	0.86	1.84	1.98
K(μg g^{-1})	0.38	0.84	0.55	0.79	8.44
Li(μg g^{-1})	1.77	0.95	0.94	0.64	0.32
Mg(μg g^{-1})	0.21	0.15	0.06	0.11	0.34
Mn(μg g^{-1})	0.04	0.12	0.77	0.03	0.09
Na(μg g^{-1})	0.21	0.49	0.27	0.08	0.27
Ni(μg g^{-1})	0.01	0.06	0.06	0.09	0.11
Ti(μg g^{-1})	5.11	2.82	5.52	3.35	17.91
SiO_2(%)	99.997	99.997	99.997	99.995	99.994

3.4 Analysis of five quartz concentrate burning and melting test results

Detailed chemical analyses and fusion tests were conducted on the five quartz

samples to evaluate their quality and suitability for practical applications [37]. As shown in Fig. 8, the transparency of the glass tubes produced from the samples varied significantly. The glass tube made from Sample No.1 and No.3 exhibited the highest transparency, indicating superior quality. In contrast, the glass produced from Sample No.2 contained numerous bubbles, which significantly reduced its transparency. Glass tubes from Samples No.4 and No.5 were filled with bubbles and displayed almost no transparency, reflecting their lower quality.

The results show that the glass quality varies significantly from Sample No.1 to Sample No.5, correlating with the inclusion content of each sample. Sample No.1 and No.3, with fewer inclusions, produced glass with higher transparency after melting. Sample No.2, which had a higher inclusion content, resulted in glass with reduced transparency. Samples No.4 and No.5, containing a large number of inclusions, produced glass that was almost entirely opaque.

Interestingly, although the SiO_2 content of Samples No.2 and No.3 was identical in the chemical composition analysis, the glass from Sample No.3 was significantly more transparent. This difference can be attributed to the lower inclusion content and impurities in Sample No.3 compared to Sample No.2. These findings confirm that inclusion content is a critical factor in determining the quality of quartz and its suitability for producing high-transparency glass. In addition to the difference in impurity content, the content of H_2O and CO_2, which are hard to measure, is also an important reason for the difference in the transparency of the glass after firing and melting between samples No. 2 and No. 3.

In summary, the inclusion analysis of the original quartz ore reveals that Sample No.1 has fewer inclusions and is classified as Class B quartz. Sample No.2 and No.3 are rated as Class C quartz, though it contains slightly more inclusions. Specifically, Sample No.3 has 3% more transparent grains and 2% fewer opaque grains compared to Sample No.2, while the proportion of semi-transparent grains is similar between the two. Component testing shows that both samples have a high SiO_2 content of 99.997% and low levels of impurity elements, meeting the standards set by Müller (2012) for high-purity quartz in Norwegian deposits. These samples also meet the

requirements for domestic high-end quartz products. Melting tests further confirm the superior quality of Sample No.1 and No.3, which produces transparent glass, whereas the glass from Sample No.2 has reduced transparency due to its higher inclusion content.

In contrast, Samples No.4 and No.5 contain a higher number of inclusions and are classified as Class D quartz. Component testing reveals lower SiO_2 contents of 99.995% in Sample No.4 and 99.994% in Sample No.5, along with higher levels of impurity elements. These impurity levels exceed the standards for high-purity quartz established by Müller (2012), making them unsuitable for high-purity quartz applications. Melting tests confirm their lower quality, as the glass tubes produced from these samples are filled with bubbles and lack transparency

Class C quartz ores, such as Samples No.2 and No.3, show potential for further purification to meet high-purity quartz standards. Optimizing the purification process may enhance their purity, enabling them to meet industrial application requirements. Inclusion recognition offers an efficient method for rapidly assessing quartz ore quality, allowing for quick and reliable evaluation of quartz deposits and their suitability for beneficiation and high-purity quartz production.

Fig. 8. Morphology of glass tubes after firing with five different quartz concentrates (Samples 1,3, 2, 4, and 5 from left to right).

4. Conclusion

This study analyzed various types of quartz ores, including white granite, pegmatite, and quartz veins, to evaluate their potential as high-purity quartz resources. A statistical analysis of inclusion content in the quartz samples was conducted, and a grading classification system was established based on grain transmittance rates. The purification process was applied to five quartz ore samples, and their impurity element content was thoroughly analyzed. The results show that quartz samples with fewer inclusions, such as Sample No.1 classified as Class B quartz, had the lowest inclusions of the five samples and was purified to have the least amount of impurities, reaching a 4N7 grade. Sample No.2 and Sample No.3 (classified as Class C quartz), achieved higher purity after purification, reaching the 4N7 grade. This meets the standards for high-purity quartz. In contrast, Samples No.4 and No.5, classified as Class D quartz, had higher inclusion content. Although their SiO_2 content reached 99.995% and 99.994%, respectively, meeting the requirements for domestic mid- to high-purity quartz, excessive levels of Al in Sample No.4 and Ti in Sample No.5 prevent them from meeting international standards for high-purity quartz. Melting test results further validated these findings. Samples with fewer inclusions and higher transmittance, such as Sample No.1, produced higher-quality glass with fewer bubbles and impurities. Conversely, the glass from Samples No.4 and No.5 was filled with bubbles and exhibited poor transparency, reflecting their lower quality. This study demonstrates that the identification and analysis of inclusions provide an efficient method for rapidly assessing quartz deposit quality. This approach offers a practical and reliable tool for exploring high-purity quartz resources in China, contributing significantly to the strategic supply of high-purity quartz materials.

Declaration of Competing Interest

The authors declare that they have no known competing financial interests or personal relationships that could have appeared to influence the work reported in this paper.

Acknowledgments

This work is supported by the Consulting Research Project of the Chinese Academy of Engineering (2024-XBZD-10, 2024-XZ-20).

References:

[1] H.L. Long, D.Q. Zhu, J. Pan, S.W. Li, C.C. Yang, and Z.Q. Guo, Advanced processing techniques and impurity management for high-purity quartz in diverse industrial applications, *Minerals*, 14(2024), No. 6, p. 573.

[2] L. Wang, C.X. Li, Y. Wang, and D.Q. Yin, China technologies present of high-purity quartz processing and the development propositions, *J. Mineral. Petrol.*, 31(2011), p. 110-114.

[3] X.D. Pan, S.Q. Li, Y.K. Li, P.H. Guo, X. Zhao, and Y.S. Cai, Resource, characteristic, purification and application of quartz: a review, *Miner. Eng*., 183(2022), p. 107600.

[4] J.C. Li, Y.Z. Li, and H.L. Kong, Current situation and development suggestions of China's high-purity quartz industry chain, *Northwest. Geol*., 56(2023), No. 5, p. 214.

[5] K.I. Vatalis, G. Charalampides, S. Platias, and N.P. Benetis, Market developments and industrial innovative applications of high purity quartz refines, *Procedia Econ. Financ*., 14(2014), p. 624.

[6] S.S. Pathirage, P.V.A. Hemalal, L.P.S. Rohitha, and N.P. Ratnayake, Production of industry-specific quartz raw material using Sri Lankan vein quartz, *Environ. Earth Sci.*, 78(2019), No. 3, p. 58.

[7] M. Xia, X.Y. Yang, and Z.H. Hou, Preparation of high-purity quartz sand by vein quartz purification and characteristics: A case study of Pakistan vein quartz, *Minerals*., 14(2024), No. 7, p. 727.

[8] C. Ma, A.S. Feng, C.M. Liu, W.H. Shao, and P. Zhao, Mineralogical characteristics and progress in processing pechnology of raw materials of high purity quartz, *Conserv. Util. Miner. Resour*, 39(2019), No. 6, p. 48-57.

[9] L. Wang, H.Z. Wang, and Y.X. Wang, Pure as Agate, Precious as a crown jewel - interpreting high

purity quartz, *Scientific and Cultural Popularization of Natural Resources*, 3(2024), p. 4.

[10] M. Lin, Z.Y. Liu, Y. Wei, B. Liu, Y. Meng, H. Qiu, S.M. Lei, X. Zhang, and Y.B. Li, A critical review on the mineralogy and processing for high-grade quartz, *Mining Metall Explor*, 37(2020), No. 5, p. 1627-1639.

[11] T. Gotoh, and M. Zhu, Quantitative evaluation of low-concentration OH impurities in quartz glass by infrared photothermal deflection spectroscopy, *Jpn. J. Appl. Phys.*, 62(2023), No. 7, p. 071004.

[12] M.A. Korekina, and A.N. Savichev, Potential of milky quartz from the Larino deposit in the Southern Urals in production of high-purity quartz concentrates, *J. Min. Sci.*, 59(2023), No. 1, p. 157.

[13] H.B. Zhao, Q. Zhang, Y. Zhang, H.J. Wang, F. Zhang, C. Ma, P.R. Lv, and L.K. Zhu, A review of the impurity element chemistry and textures of natural quartz and its application to the prospect of high purity quartz deposit, *Northwest. Geol.*, 57(2024), No. 5, p. 106-119.

[14] A. Müller, J.E. Wanvik, and P.M. Ihlen, Petrological and chemical characterisation of high-purity quartz deposits with examples from Norway, *Mineral. Anal.*, (2012), p. 71-118.

[15] L. Wang, Concept of high purity quartz and classification of its raw materials, *Conserv. Util. Miner. Resour,* 42(2022), No. 5, p. 55.

[16] Y.P. Xie, S.Q. Li, X.D. Pan, Y.K. Li, and A. Zhang, Recent advances in the marketing, impurity characterization and purification of quartz, *Miner Miner Mater*, 2(2023), p. 16.

[17] M. Lin, S.Q Xu, Z.Y. L, Y. Wei, B. Liu, Y. Meng, H. Qiu, and S.M. Lei, Review for high-purity quartz (SiO_2) (Part Ⅲ): Analysis, activation and separation of fluid inclusions, *Multipurp. Util. Miner. Resour.*, 43(2022), No. 6, p. 26-29.

[18] S.J. Wang, D.S. Yu, C. Ma, F.S. Wei, and H.Q. Zhang, A new insight into the influence of fluid

inclusions in high-purity quartz sand on the bubble defects in quartz glass: A Case Study from Vein Quartz in the Dabie Mountain, *Minerals*, 14(2024), No. 8, p. 794.

[19] Z.C. Hu, Z.G. Yu, T. Zhao, D.G. Ding, X. Lv, Y.S. Ji, L.H. Peng, D.R. Yang, and X.G. Yu, Study on the mechanism of second phase formation in high-purity fused silica materials for semiconductor application, *J. Non-Cryst. Solids*., 635(2024), p. 122990.

[20] A. Aliasgharzadeh-Polesangi, H. Abdollah-Pour, and Y. Alizad Farzin, Nanostructured silicon production from quartzite ore by low-energy wet blending of the reagents, reduction in controlled atmosphere, and hydrometallurgy, J. Mater. Res. *Technol*., 8(2018), No. 1, p. 1014-1023.

[21] Q. Deng, Z.J. Ren, Y.H. Song, Y.H. He, P.Y. Li, and H. Yin, Purification of different-sized quartz crystals in granitc pegmatite, *Miner. Eng*., 216(2024), p. 108856.

[22] G. Zhou, H.J Sun, and T.J. Peng, Exploration of the correction between Na_2CO_3 fluxing agent and crystal phase transformation and mechanical properties of asbestos tailings microcrystalline ceramics, *MR*, 35(2021), No. 7, p. 7013-7018.

[23] Y.K. Li, S.Q. Li, X. Zhao, X.D. Pan, and P.H. Guo, Separation and purification of high-purity quartz from high-silicon iron ore tailing: An innovative strategy for comprehensive utilization of tailings resources, *Process Saf. Environ. Prot*., 169(2023), p. 142-148.

[24] Y.Z. Feng, Y. Zhang, Y.L. Xie, Y.J. Shao, H.J. Tan, H.B. Li, and C.K. Lai, Ore-Forming mechanism and physicochemical evolution of gutaishan Au deposit, South China: Perspective from quartz geochemistry and fluid inclusions, *Ore Geol. Rev*., 119(2020), p. 103382.

[25] R.Y. Zhang, C.H. Tang, W. Ni, J. Yuan, Y. Zhou, and X.L. Liu, Research status and challenges of high-purity quartz processing technology from a mineralogical perspective in China, *Minerals*, 13(2023), No. 12, p. 1505.

[26] M. Lin, Z.Y. Pei, and S.M. Lei, Mineralogy and processing of hydrothermal vein quartz from Hengche, Hubei Province (China), *Minerals*, 7(2017), No. 9, p. 161.

[27] E. Larsen, R.A. Kleiv, Flotation of quartz from quartz-feldspar mixtures by the HF method, Miner., (98)2016, p. 49-51.

[28] B.A. Gaweł, A. Ulvensøen, K. Łukaszuk, A.M.F. Muggerud, and A. Erbe, In situ high temperature spectroscopic study of liquid inclusions and hydroxyl groups in high purity natural quartz, *Miner. Eng.*, 174(2021), p. 107238.

[29] H.Y. Zhou, A. M ü ller, and J. Berndt, Quartz chemistry fingerprints melt evolution and metamorphic modifications in high-purity quartz deposits, *Geochim. Cosmochim. Acta*, 356(2023), p. 179-195.

[30] Q.L. Hou, C. P.F. Chen, L. Tian, and J.K. Xiao, Study on crack mechanism of gas-liquid inclusions in quartz sand under microwave heating, *E3S Web Conf.*, 248(2021), p. 8.

[31] B.A. Gaweł, A. Ulvensøen, K. Łukaszuk, B. Arstad, A.M.F. Muggerud, and A. Erbe, Structural evolution of water and hydroxyl groups during thermal, mechanical and chemical treatment of high purity natural quartz, *RSC Adv.*, 10(2020), No. 48, p. 29018-29030.

[32] X.F. Chen, X.C. Wang, and X.Z. Fu, Hierarchical macro/mesoporous TiO_2/SiO_2 and TiO_2/ZrO_2 nanocomposites for environmental photocatalysis, *Energy Environ. Sci.*, 2(2009), No. 8, p. 872-877.

[33] X. Zhong, S. Royer, H. Zhang, Q.Q. Huang, L.J. Xiang, S. Valange, and J. Barrault, Mesoporous silica iron-doped as stable and efficient heterogeneous catalyst for the degradation of C.I. acid orange 7 using sono–photo-fenton process, *Sep. Purif. Technol.*, 80(2011), No. 1, p. 163-171.

[34] Q.L. Hou, J. Li, R.M. Yin, L.Z. Chen, L. Li, and F.B. Ji, Study on gas-liquid inclusions in quartz

sand under microwave field, *Adv. Mater. Res.*, 581(2012), p. 689-693.

[35] K.X. Wei, H.W. Zhang, W.H. Ma, S.J. Guo, and D.D. Wu, Research progress on preparation technology of high purity quartz sand, *Journal of Kunming University of Science and Technology(Natural Science)*, 45(2020), No. 6, p. 9-20.

[36] R. Thomas, and P. Davidson, The Missing link between granites and granitic pegmatites, *J. Geosci.*, 58(2013), No. 2, p. 183-200.

[37] Q.L. Ma, Z.Y. Liu, Y.H Zhong, Y.D Lang, X.Z Liu, and H.S. Fang, Thermal optimization of induction-heated pulling-down furnace for quartz glass rod fabrication, *Appl. Therm. Eng.*, 141(2018), p. 1-9.